We are IntechOpen, the world's leading publisher of Open Access books Built by scientists, for scientists

4,800
Open access books available

122,000
International authors and editors

135M
Downloads

Our authors are among the

154
Countries delivered to

TOP 1%
most cited scientists

12.2%
Contributors from top 500 universities

CLARIVATE ANALYTICS BOOK CITATION INDEX INDEXED

WEB OF SCIENCE™

Selection of our books indexed in the Book Citation Index in Web of Science™ Core Collection (BKCI)

Interested in publishing with us?
Contact book.department@intechopen.com

Numbers displayed above are based on latest data collected.
For more information visit www.intechopen.com

1

Thermodynamics of Molecular Recognition by Calorimetry

Luis García-Fuentes, Ramiro, Téllez-Sanz,
Indalecio Quesada-Soriano and Carmen Barón
University of Almería, Almería
Spain

1. Introduction

When Otto von Guericke, stimulated by the previous work of Galileo and Torricelli, constructed the world's first-ever vacuum pump in 1650 to disprove Aristotle's supposition that "nature abhors a vacuum", he could not imagine the newly-born scientific field would get us closer to understand one of the oldest questions in the history of mankind: what is life?. Even though nobody is able to answer this question correctly yet, thermodynamics helps us to address another one, equally important: how does it work? The cellular machinery is a highly complex system, probably the most complex ever created by nature. A perfect gear with thousands of chemical reactions taking place synchronously requiring high efficiency enzymes, which are responsible for providing the cell in time with the products it needs. One of the basic aims of the biophysical research is to be able to control how enzymes work. But there's no possible control if you don't previously understand how the molecular recognition between ligand and protein occurs and how favorable it is.

Thermodynamics is the only scientific field allowing to address the matter. Any molecular recognition process, as a chemical reaction, is associated with a change in the molecular properties of the reactants. Understanding the molecular recognition processes between small ligands and biological macromolecules takes a complete characterization of the binding energetic, as well as the correlation between thermodynamic data and chemical structure. Techniques such as fluorimetry, spectrophotometry or circular dichroism are convenient, fast and low sample-consuming, but their application is not universal.

However, there is such a universal technique, the Isothermal Titration Calorimetry (ITC), standing above the others. Modern isothermal titration calorimeters (e.g. VP-ITC or iTC-200 from Microcal (http://www.microcal.com/) and nano ITC (http://www.tainstruments.com/) are able to measure the energetic of ligand binding (for example, a drug) in a highly reliable, fast and accurate way, using relatively small amounts of material. Typically, these calorimeters require less than 500 μg of protein per complete calorimetric titration and can measure heat effects as small as 0.1 μcal, thus allowing the determination of binding constants as large as 10^8 to 10^9 M^{-1}. Chemical interaction changes are always associated with a heat energy exchange with the environment. This fact turns ITC, among the possible choices, in the safest bet to address these studies. In an ITC experiment the heat

evolved when two reactants are mixed is monitored as a titration curve where one of them, frequently the macromolecule, is titrated at constant temperature against the ligand. Planning and careful performing the experiments is crucial to get quality data from which extracting reliable thermodynamic parameters and interpretations. ITC is currently used in a large number of molecular recognition studies, such as antigen-antibody, protein-peptide, protein-protein, sugar-protein, DNA-protein and protein-ligand studies, as well as enzyme kinetics.

The quantitative analysis of the molecular association driving forces between a biological macromolecule and a ligand requires the determination of thermodynamic parameters. The suitability of ITC lays on its ability to not only providing the affinity, usually expressed in terms of the association constant, but also the enthalpic (ΔH) and entropic (ΔS) contributions to the Gibbs free energy of association ($\Delta G=\Delta H-T\Delta S$). Under right conditions, a single ITC experiment is able to give the values for these changes along with the stoichiometry or number of binding sites (n). Moreover, in the cases in which more than one binding site is present, it is also possible to examine the sites for cooperativity.

Each interaction, either hydrophobic, pi-stacking, electrostatic, proton release or uptake... has its own energetic fingerprint. Splitting the global energetics into individual contributions is the key to know, with a great deal of reliability, details such as which enzyme residue is involved in a proton uptake or which other locks the ligand into position through a pi-stacking. This assignment of individual residue roles would not be possible without the calorimetric study of some protein mutants, obtained by directed mutagenesis. It is also important to have structural information about the complexes. When X-ray crystallographic data is not available, molecular docking studies can replace it as long as it is used with enough precaution and the user has previous structural knowledge from similar ligands.

The combination of different protein-ligand binding experiments performed under different solution conditions allows for other parameters to be calculated. For instance, the heat capacity change (ΔC_p) can be determined through a temperature change. ΔC_p is closely related to, among other factors, changes in the solvent Accessible Surface Areas (ASA's) upon complex formation. Or, when a change in the protonation state of one of more groups accompanies the complex formation, the number of protons uptaken or released can be determined from a series of experiments carried out with different buffers or at different pH values. ITC is, thus, a key tool to elucidate which chemical structures a ligand must possess to bind a protein with high affinity and specificity. Since this is the main requirement for a rational drug design against a biological target, ITC is a valuable technique for identifying and optimizing molecules with therapeutic properties.

The chapter will deal, through experimental results, with the necessary requirements for a complete thermodynamic protein-ligand binding study allowing for the maximal amount of information to be obtain about the molecular recognition basis: how to plan the experiments, data analysis, strategies to follow to overcome difficulties and the splitting of energetic parameters into individual contributions.

2. Background of binding thermodynamic

For a simple reversible bimolecular binding reaction between a target macromolecule (M) and a ligand (X), represented as:

$$M + X \rightleftarrows MX \tag{1}$$

the change in the Gibbs free energy (ΔG), for the ligand-macromolecule complex formation of the complex (MX) is related to the standard Gibbs free energy change (ΔG^o), by the equation:

$$\Delta G = \Delta G^0 + RT \ln\left(\frac{[MX]}{[M][X]}\right) \tag{2}$$

At equilibrium, under standard conditions, when ΔG=0, this becomes:

$$\Delta G^0 = -RT \ln\left(\frac{[MX]}{[M][X]}\right) = -RT \ln K_a = RT \ln K_d \tag{3}$$

where K_a is the equilibrium association constant, commonly named as affinity, and K_d is the dissociation constant. Moreover, the binding parameter, ν, is defined as the ratio between the concentrations of bound ligand, $[X]_b$ and the total macromolecule, $[M]_t$:

$$\nu = \frac{[X]_b}{[M]_t} = \frac{[MX]}{[M]_t} = \frac{[MX]}{[MX]+[M]} = \frac{K_a[X]}{1+K_a[X]} = \frac{[X]}{K_d+[X]} \tag{4}$$

K_a or K_d can be measured using a great variety of experimental techniques (fluorescence, circular dichroism, equilibrium dialysis, surface plasmon resonance, etc.). However, a complete thermodynamic characterization requires the enthalpy change, which accounts for the heat exchange during the association reaction, to be measured. When this is done, the entropic contribution to the overall observed Gibbs free energy can be calculated through the relationship $\Delta G^0=\Delta H-T\Delta S^0$ (assuming that $\Delta H=\Delta H^0$). The sign and value of the observed enthalpy are the global result of the interaction changes taking place at binding time: their type and number, bond length and angle changes… but perhaps the most important contribution, enthalpically speaking, is the hydrogen bonding. Thus, the sign indicates if there is a net favorable (negative) or unfavorable (positive) redistribution of the hydrogen bond network between the reacting species, including the solvent. The entropy change can be related to the relative degree of disorder after binding. For instance, the release of water molecules to the bulk solvent is a source of favorable entropy. Thus, hydrophobic interactions are characterized by a small enthalpy (negative or positive), and a favorable entropy. Thus, two interactions with similar affinities and structures can have different enthalpic and entropic contributions to the Gibbs free energy of binding.

Enthalpy changes can be measured in an indirect way through the integrated form of the van't Hoff equation. However, this is done under the assumption that ΔH^o is constant within the studied temperature range, which is seldom the case. ITC is by far the preferred method, since it provides a direct and accurate measurement at every temperature. There are reported discrepancies between calorimetric and van't Hoff enthalpies (Horn et al., 2001), proving the advantage of using ITC to determine enthalpy changes.

3. General aspects of ITC

3.1 Instrumentation

The basic design of ITC instruments has scarcely changed over the last 10 years. The most modern instruments operate a differential cell feedback system, where the reference cell is filled with water or buffer and the sample cell usually contains the macromolecule. A syringe that also serves as the stirrer adds the ligand in a stepwise fashion at preset intervals during the course of the experiment. Heat produced or absorbed during the binding reaction is monitored as a temperature change. Any temperature difference between the sample and reference cells triggers a feedback system which modulates the applied thermal power in order to keep the temperature difference between both cells as low as possible. The instrument slowly increases the temperature of both cells during each titration (less than 0.1 ^{o}C per hour), in a way that approximates isothermal conditions. Usually cell volumes are around 1.5 mL, the thermostat temperature can be set between 5 and 80 ^{o}C, and heats as small as 0.1 μcal can be measured.

3.2 Experimental planning

The setup of an ITC experiment is largely dependent on the thermodynamic characteristics of the system of interest, i.e., the expected binding affinity and the heat effect of the interaction. To obtain high quality data, an appropriate protocol has to be established by optimizing ligand and protein concentrations, the injection volume and the values of K, ΔH, and n (or a larger set of parameters for binding models other than the n equal and independent binding sites). The shape of the binding curve is dependent on the C-value, defined this, as product of the association constant K_a and the sites molar concentration of the macromolecule $[M]_T$ being titrated (Wiseman et al, 1989). This value is crucial for an accurate determination of the binding parameters. Experience shows that for a good ITC experimental design (sigmoidal termogram) a C-value in the 10-100 range should be chosen. However, in many cases, the intrinsic properties of the system avoid reaching a good C-value, and it is up to the user to choose the more adequate experimental conditions. Clearly, simulations are important in optimizing an ITC experiment and in achieving a balance between detectable heats and thermogram curvature.

As an example, we will use the binding of dUDP to trimeric dUTPase from *Plasmodium falciparum* (PfdUTPase) in glycerophosphate buffer at pH 7 and 25 ^{o}C (Quesada-Soriano et al., 2007). Fig. 1 shows a typical calorimetric titration. What is needed to reach such an experimental outcome?. As indicated above, the appropriate concentration range for the macromolecule placed in the cell depends on the binding constant. Since in this case the approximate value for the binding constant at 25 ^{o}C is $K_a = 6 \cdot 10^5$ M^{-1}, with a stoichiometry of 3 mol of ligand per mol of trimeric enzyme, a concentration of macromolecule of approximately 20 μM yields a C-value of 36, within its ideal 10-100 range. The actual value was 22.7 μM.

The macromolecule in the cell is titrated with a series of small injections of the ligand solution from the syringe, the concentration of which must be much higher than that for the macromolecule in the cell since the titration experiment is planned to approach or reach complete saturation of the binding sites at the end (Fig. 1). The number and volume of the ligand injections should be chosen so that the sigmoidal shape is as well defined as possible, usually with a large number of small aliquots, between 5 and 10 μL. Only if the heat signal is small it will be necessary to choose larger injection volumes.

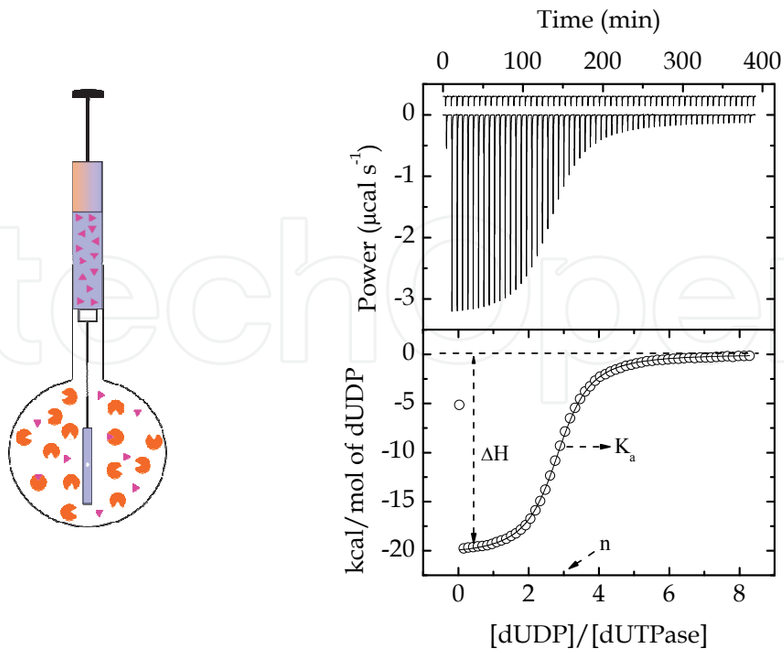

Fig. 1. Scheme of the calorimeter reaction cell (left) and results of a typical ITC experiment (right). The sigmoidal thermogram in the upper panel on the right side corresponds to the binding of a ligand (dUDP) to a trimeric protein (dUTPase). The small linear thermogram above the sigmoidal one comes from the so-called "ligand dilution experiment", where the ligand is injected into the sample cell containing just the buffer. Each thermogram consists of the heat peaks generated by a series of 5 μL injections from the syringe (containing the ligand solution) into the sample cell (containing the macromolecule or plain buffer solutions). The bottom panel shows the non-linear least squares analysis of the thermodynamic data to a suitable model, yielding the values for K_a, ΔH and n.

These requisites define the titration protocol, and it is up to the user to find the ideal compromise. In this particular example, 58 injections, 5 μL-each (preliminary 1 μl injection), of a ligand solution (dUDP) with a concentration 40 times higher than that of the protein solution will give an adequate binding isotherm. If association is fast compared to the response time of the calorimeter, and the heat signal is not very large, the instrument baseline will be recovered in a short time. In those cases, four or five minutes are usually enough to reach baseline again after injection. In Fig. 1, this time was set to about five minutes. In contrast, heat signals of slow processes, such as covalent reactions or enzymatic kinetics, require much more time to reach thermal equilibrium.

Finally, other issues, also related to experimental design, should be taking into account. It is very important that ligand and macromolecule solutions are pure and exactly each other regarding pH and solution conditions. For this reason, the macromolecule and the ligand should be are preferably dissolved in the same buffer. It is a good practice to dialyze the protein prior to the experiment and dissolve the ligand in the last dialysis buffer change. Furthermore, air bubbles have to be avoided in the sample cell. Thus, it is very important to degas, all solutions prior to the experiment during a short time. Also, any air bubble left in the syringe after filling it can cause variation in the injected volume or lead to additional heat signals. Finally, in most experiments the heat effect of the first injection of a series of

injections is obviously too small. This results from diffusion while equilibrating the system. Even if care is taken to avoid this leakage, the problem may persist. Therefore it is common practice to make a small first injection of 1 μL and then to remove the first data point before data analysis.

The result from a titration is a plot of the recorded power, dQ/dt, *vs.* time, as shown in the right upper panel of Fig. 1. Each peak represents the thermal effect associated with an injection. The right lower panel shows the integrated areas as a function of the ligand/protein molar ratio.

The heat effects after every ligand injection arise from four main sources: binding interaction, ligand dilution, macromolecule dilution and a mixing heat effect. Generally, the dialysis/dialysate approach will virtually eliminate the mixing. The dilution heat of both the macromolecule and the ligand must be measured in separate experiments. For the first, buffer is injected from the syringe into the macromolecule solution in the sample cell, whereas for the latter the ligand is injected into the sample cell containing just buffer. Since the macromolecule concentration placed in calorimetric cell is usually in the micromolar range, its dilution heat is negligible. Thus, this titration can be skipped. However, the ligand dilution heat is not always negligible and it needs to be measured in an independent titration and substrated from the injection heats measured in the binding titration (Fig. 1).

There are situations where the general procedure above is not the best choice, like when the ligand is poorly soluble. In these cases a so-called "reverse titration" may be preferred, where the macromolecule is inside the syringe and the ligand in the sample cell. The analysis procedure has to be modified accordingly, especially if the macromolecule has several binding sites.

4. Data analysis

4.1 Equal and independent binding sites model

The equal and independent binding sites model describes the simplest way a macromolecule can interact with a ligand. The system described above will be used as an example (i.e. dUDP/PfdUTPase). Structurally, *Pf*dUTPase is a trimer with three identical active sites located at the subunit interfaces. Each active site is made up by residues from all three subunits, five or which are highly conserved. For such a system the binding parameter, υ, is related to the fractional saturation, Y, by

$$\nu = n \cdot Y \tag{5}$$

where n is the number of binding sites, in this case n=3. The concentration of free ligand is related to the total ligand, $[X]_t$, and the bound ligand, $[X]_b$, by the mass conservation law:

$$[X] = [X]_t - [X]_b \tag{6}$$

By using Eqs. 4 and 5, Eq. 6 can be represented by the relationship

$$[X] = [X]_t - nY[M]_t \tag{7}$$

On the other hand, the binding constant, K_a, is given by,

$$K_a = \frac{Y}{(1-Y)[X]} \tag{8}$$

The combination of Eqs. 7 and 8 gives the quadratic equation

$$Y^2 - Y\left(1 + \frac{1}{nK_a[M]_t} + \frac{[X]_t}{n[M]_t}\right) + \frac{[X]_t}{n[M]_t} = 0 \tag{9}$$

where the only root with physical meaning is,

$$Y = \frac{1}{2}\left(1 + \frac{1}{nK[M]_t} + \frac{[X]_t}{n[M]_t} - \sqrt{\left(1 + \frac{1}{nK[M]_t} + \frac{[X]_t}{n[M]_t}\right)^2 - \frac{4[X]_t}{n[M]_t}}\right) \tag{10}$$

The accumulated or integral binding heat of the process after the i^{th} injection is given by

$$Q = n[M]_t V_0 \Delta H_t Y_i \tag{11}$$

where V_0 is the cell volume and ΔH_t is the molar enthalpy change of the binding reaction. The heat of the i^{th} injection (differential heat) is,

$$q_i = V_0 \Delta H_t \cdot \Delta[L]_b = V_0 \Delta H_t \cdot n[M]_t \left(Y_i - Y_{i-1}\right) \tag{12}$$

with $\Delta[L]_b$ being the difference in the bound ligand concentration between the i^{th} and $(i\text{-}1)^{th}$ injections. It is very important to underline that the functional form of $\Delta[L]_b$ depends on the specific binding model. Thus, for this simplest model, when the protein has n binding sites, Eq. 12 becomes

$$q_i = V_0 \Delta H_t \cdot n[M]_t \left(\frac{K_a[X]_i}{1 + K_a[X]_i} - \frac{K_a[X]_{i-1}}{1 + K_a[X]_{i-1}}\right) \tag{13}$$

The experimental titration data from Fig. 1 can be non-linearly fitted to the sigmoidal curve defined by Eqs. 7 and 13 (q_i *vs.* $[X]_t$, or *vs.* $[X]_t/[M]_t$). The model yields the values for its parameters (K_a, ΔH_t, and n) from a single experiment. In the example in Fig. 1, the parameter values obtained were n=2.85, K_a=5.7 ·10^5 M^{-1} and ΔH_t = -20.4 kcal/mol. It is worth noticing that the resulting stoichiometry differs somewhat from three (three binding sites). This discrepancy between the calorimetric determined stoichiometry and the real number of binding sites in the enzyme is very frequent and there are two main reasons for it to appear: concentration errors (ligand and/or protein) and the presence of a small fraction of damaged macromolecule unable to bind ligand. These small errors are acceptable and within experimental error, although a usual procedure is to remove the stoichiometry parameter from the fitting session by fixing it at a constant value (only if its value is known and trusted). This way only ΔH_t and K_a are calculated by the fitting procedure.

4.2 Equal and interacting binding sites model

When good quality data has been obtained but the simplest model above is unable to yield a successful fit, then it is not valid to describe the macromolecule-ligand interaction. If the macromolecule is composed of identical subunits, the next logical step is trying an equal and interacting binding sites model. This model makes the assumption that a ligand molecule binds the macromolecule with a different affinity than the previous one, i.e, there

is cooperativity. When the complexity of the model increases it is common practice to use a statistical thermodynamic approach to deduce the binding equations. However, the fitting success strongly depends on the quality of the experimental data.

To describe this model we are using experimental data from the binding of the Pi class human glutathione S-transferase enzyme to two glutathione conjugates. Human glutathione transferase P1-1 (hGSTP1-1), a homodimeric protein of ≈46 kDa, has been extensively studied for its potential use as a marker during chemical carcinogenesis and its possible role in the mechanism of cellular multidrug resistance against a number of anti-neoplastic agents (Hayes et al., 2005). S-nitroglutathione (GSNO) binds to wild-type hGSTP1-1 with negative cooperativity, whereas the C47S mutation induces positive cooperativity towards both GSNO and (ethacrynic and glutathione conjugate) EASG binding (Tellez-Sanz et al., 2006; Quesada-Soriano et al., 2009).

The equilibrium between a ligand and a macromolecule with two ligand binding sites can be described in terms of two different sets of association constants: the macroscopic association constants (overall, β_i, or stepwise, K_i), or the microscopic or intrinsic constants:

$$\beta_1 = K_1 = \frac{[MX]}{[M][X]}; \quad \beta_2 = \frac{[MX_2]}{[M][X]^2} = K_1 \cdot K_2 \tag{14}$$

The microscopic binding constants, K_i^0, are related to the intrinsic ligand binding to a site, and therefore reflect the intrinsic binding affinities to each site. The relationship between macroscopic and microscopic binding constants is a statistical factor given by

$$K_i = \frac{n-i+1}{i} K_i^0 \tag{15}$$

Therefore, for the two interacting sites case, there are two microscopic constants, one per site ($K_1^0=1/2K_1$ and $K_2^0=2K_2$), and the binding parameter or Adair´s equation, ν, will be given by

$$\nu = \frac{2K_1^0[X] + 2K_1^0K_2^0[X]^2}{1 + 2K_1^0[X] + K_1^0K_2^0[X]^2} \tag{16}$$

The denominator in Eq. 16 is called the binding polynomial, P, or binding partition function and it represents the sum of the different macromolecular species concentrations relative to that of the free macromolecule that is taken as the reference:

$$P = \sum_{i=0}^{n} \frac{[MX_i]}{[M]} \tag{17}$$

which with two sites (n=2), and using Eqs. 14 and 15, the expression shown in the denominator of Eq. 16 is deduced.

The free ligand concentration is related to the total ligand $[X]_t$ and the bound ligand, $[X]_b$ by

$$[X] = [X]_t - [X]_b = [X]_t - [M]_t \left(\frac{2K_1^0[X] + 2K_1^0K_2^0[X]^2}{1 + 2K_1^0[X] + K_1^0K_2^0[X]^2} \right) \tag{18}$$

The accumulated or integral binding heat of the titration after the ith injection is given by

$$Q = V_0[M]_t \left[\frac{2K_1^0 \Delta H_1[X] + K_1^0 K_2^0 (\Delta H_1 + \Delta H_2)[X]^2}{1 + K_1^0[X] + K_1^0 K_2^0[X]^2} \right] \tag{19}$$

where ΔH_1 and ΔH_2 will be the binding enthalpy changes for the first and second site, respectively. These expressions are completely general for any macromolecule with two interacting ligand-binding sites, irrespective of positive or negative cooperativity. Consequently, the heat of the ith injection is,

$$q_i = Q_i - Q_{i-1} \tag{20}$$

When a system behaves according to this model, a nonlinear fit using Eqs. 18, 19 and 20 can fit the titration data (q_i vs. $[X]_t$, or vs. $[X]_t/[M]_t$). Fig. 2 (left panel) shows a typical ITC profile for the binding of GSNO (12.7 mM) to dimeric wt-hGSTP1-1 (43.7 μM) in phosphate buffer at pH 7.0 and 25°C. Control experiments were also carried out in order to measure the ligand dilution heat. A noncooperative model is unable to fit these calorimetric data properly.

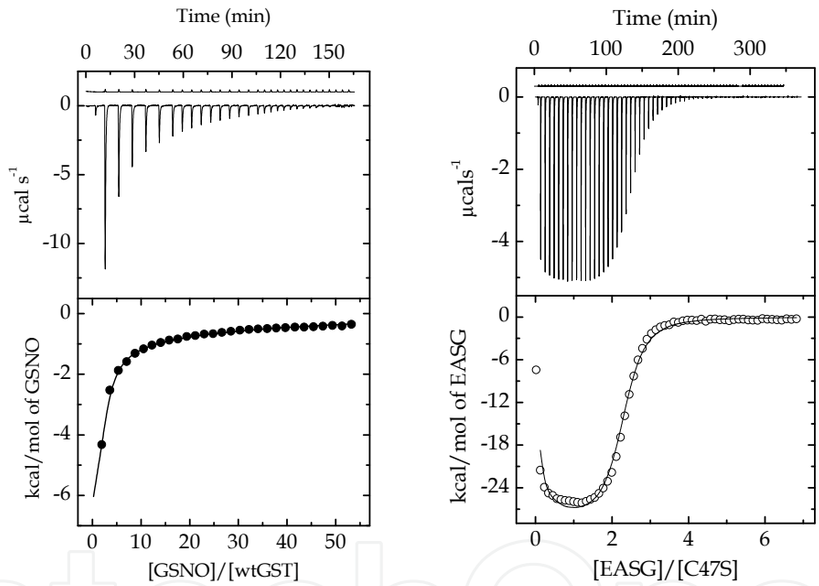

Fig. 2. Representative isothermal titration calorimetry measurements for the binding at 25.1 °C of GSNO (left panel) and EASG (right panel) to wt-hGSTP1-1 and its C47S mutant, respectively. Solid lines in the bottom plots represent the fit to an equal and interacting binding sites model.

The calculated parameters for the left panel in Fig. 2 by an iterative fitting procedure were: (K_1^0=7.0±0.4) ·10^4 and K_2^0= (2.3±0.2) ·10^3 M^{-1}; ΔH_1=-7.9±0.8 and ΔH_2=-24.8±0.7 kcal/mol. Thus, the intrinsic binding constant value for the first site, K_1^0, is higher than that for the second site, K_2^0, and consequently ligand binding induces negative cooperativity in the enzyme. Right panel in Fig. 2 shows the binding of EASG (1 mM) to the C47S mutant (33 μM) of hGSTP1-1. From a closer inspection of both thermograms, it is clear the ligand binds in a different way to the wild-type (left panel) than to the C47S mutant (right panel). For the right panel, the calculated parameter values are: K_1^0=(4.9±0.3) ·10^4 and K_2^0= (1.2±0.1) ·10^6 M^{-1}; ΔH_1=-1.8±0.1 and ΔH_2=-58.5±0.2 kcal/mol. In this case, the microscopic binding constant for

the first site is lower than that for the second site. This result indicates the binding of EASG to the first subunit induces a favorable conformational change on the second one, which in turn displays an increased affinity for EASG (positive cooperativity).

4.3 Others binding models

The procedure described above is suitable for deducing the equations for other models such as multiple sets of independent sites, multiple sets of interacting sites,… However, in all of these cases the model to fit the data to must be known or suspected in advance.

There exists a general formalism to analyze many experimental biological systems involving ligand binding that can be used when the user has no hint about which model to choose: the theory of the binding polynomial (Freire et al., 2009). It allows the analysis of experimental data by employing a general model-free methodology that provides essential information about the system, such as whether there exists binding cooperativity, if it is positive or negative or the magnitude of the cooperativity energy. The binding polynomial contains all the information about the system and allows derivation of all the thermodynamic experimental observables. Consequently, when the model to fit the data is not known, this method is the preferred starting point for the analysis of complex binding situations.

Another situation requiring a special approach to analyze the data is when the ligand binding to the protein is so tight that the high association constant value cannot be measured directly by one ITC experiment. In this case, a displacement titration can solve the issue. It consists of a regular binding experiment where the protein in the cell is premixed with a weaker competitive ligand. Three titrations must be carried out: a direct titration of the high-affinity ligand to the target protein, a direct titration of the weak ligand to the target protein and a displacement titration of the high-affinity ligand to the weak ligand-target protein complex (Velazquez-Campoy & Freire, 2006).

4.4 Data kinetic analysis

ITC also provides a direct and accurate method for determining the kinetic parameters of a chemical reaction when its observed kinetic constant is smaller than the calorimeter response time, from the heat absorbed or released during the reaction. Thus, it is a valid method for some enzyme catalyzed processes.

There are two different scenarios: when the binding heat evolved is negligible compared to that of the chemical reaction, and when both are of a similar magnitude.

4.4.1 Measurement of kinetic parameters by ITC when the binding heat is negligible

This is the case when the enzyme is present at catalytic concentrations. ITC provides a direct and accurate assay for determining kinetic parameters of an enzyme catalysed reaction, based on the measurement of the heat absorbed or released during the catalytic reaction. Frequently, two procedures are employed: multiple injections or the continuous method (Todd & Gomez, 2001). Although the two methods provide analogous results, the use of one or the other depends on the particular characteristics of the reaction under study. However, as a rule of thumb, the multiple injection assay is recommended when the K_m value is greater than 10-15 μM, leaving the continuous assay for when $K_m < 10$ μM.

As an example we describe the methodology and data analysis to obtain the kinetic parameters for the PfdUTPase enzyme. dUTPase catalyzes the hydrolysis of α-β-pyrophosphate bond of dUTP to yield dUMP and inorganic pyrophosphate (PP_i). This

hydrolysis reaction releases protons and typically is studied spectrophotometrically in a coupled assay by using a pH indicator in a weak buffered medium with similar pK_a. However, the ITC method proved to be more sensitive, even detecting the activity in the case of some mutants where the spectrophotometric method was unable to detect it.
Briefly, the ITC method for enzyme assays is based on the fact that the thermal power reflects the heat flow (dQ/dt). This thermal power or heat flux (μcal·s^{-1}) is directly proportional to the rate of product formation or substrate deflection and can be described as

$$v = d[P]/dt = \frac{dQ}{dt} / \Delta H_{obs} V_0 \tag{21}$$

where V_0 is the effective volume of the calorimetric cell, and Q and t are values measured during the experiment. ΔH_{obs} is the observed molar enthalpy for the conversion of substrate to product. Fig. 3 shows a typical experimental thermogram (using the continuous method also termed as "single injection assay") for the titration of PfdUTPase with dUTP in the presence of 25 mM $MgCl_2$ at pH 7 and 25.2 °C (Quesada-Soriano et al., 2008).

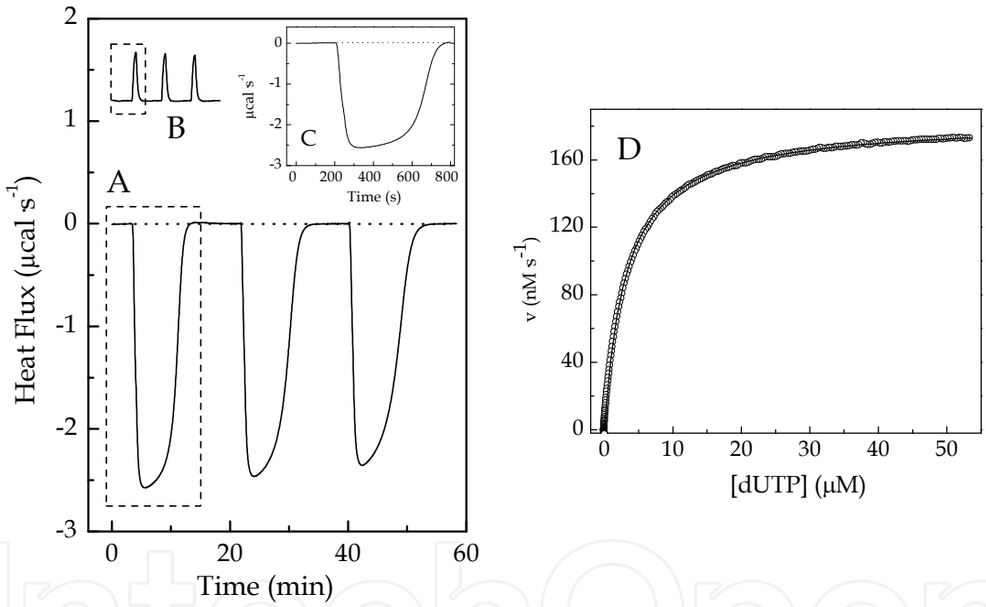

Fig. 3. PfdUTPase-catalyzed hydrolysis of dUTP in 25 mM MES, 100 mM NaCl, 25 mM $MgCl_2$, 1 mM β-mercaptoethanol at pH 7 and 25 °C. (A) Typical calorimetric trace (μcal/s versus time) obtained after addition of three injections of 5 mM dUTP (20 μl) to the calorimetric cell containing PfdUTPase (5.3 nM). (B) dUTP dilution thermogram. (C) Calorimetric trace (first injection) resulting after subtracting the first peak of the dilution experiment. (D) Net thermal power was converted to rate and fitted to the Michaelis–Menten equation, giving ΔH_{obs} = − 10.4 kcal/mol, K_m = 3.2 μM, k_{cat} = 11.7 s^{-1}.

It is very important to observe that the response time of the calorimetric signals when a kinetic process occurs is much higher than in a typical binding process. In this way, the catalyzed reaction progress can be followed from analysis of the calorimetric peaks (first or second injections). Thus, the reaction rate can be calculated since the heat flow (dQ/dt) is directly proportional to the rate of reaction (Eq. 21). The area under each peak gives the

total heat for the reaction (Q_T) which is converted to ΔH_{obs} (cal/mol) by means of the expression

$$\Delta H_{obs} = \left(-\int_0^{\infty} (dQ / dt)dt \right) / V_0[S]_0 \tag{22}$$

where $[S]_0$ is the initial substrate concentration, and in this example $[dUTP]_0$. The downward displacement of the baseline after the substrate injection indicates the exothermic nature of the reaction. On the other hand, the substrate concentration in any time $[S]_t$ was calculated by the expression

$$[S]_t = [S]_0 - \left(\int_0^{t} (dQ / dt)dt \right) / V_0 \Delta H_{obs} \tag{23}$$

Fig. 4, shows the raw data for thermal power change as a function of time in the multiple injections assay for the hydrolysis process of dTTP by human dUTPase (Quesada-Soriano et al., 2010).

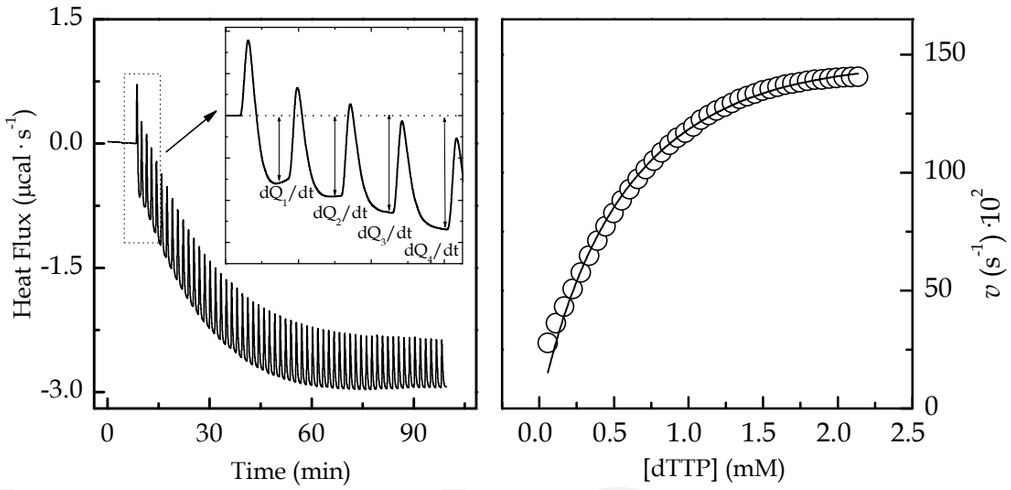

Fig. 4. Raw data for thermal power change as a function of time in the multiple injections assay for the hydrolysis process of dTTP by human dUTPase (left panel). The non-linear least squares fits of the experimental data to the Michaelis–Menten equation (right panel). Kinetic assays were performed in 25 mM MES, 5 mM NaCl, 1 mM β-mercaptoethanol and 25 mM $MgCl_2$ (pH 7, 25 °C), making 5 μL injections of 15 mM substrate into calorimetric cell containing 15–25 μM enzyme.

Briefly, this method measures the rate of enzyme catalysis during stepwise increase of substrate concentration in an enzyme solution. After initial equilibration, as a result of the deoxynucleoside triphosphate injections (5 μL each), an initial endothermic peak corresponding to the heat dilution was generated. The baseline then stabilises at a lower power level than those of the previous injections as a consequence of the heat generated by the enzymatic reaction and due to the fact that the higher the substrate accumulation, the faster the reaction occurs. The drop in baseline also indicates that this particular reaction proceeds with a negative (exothermic) enthalpy. Values of rate determined in this way will yield data

into units of μcal per second. These can be readily converted in units of molar per second using Eq. 21 and the ΔH_{obs} value. Thus, in the kinetic experiments using the stepwise injection method is need to perform an additional experiment using a higher enzyme concentration in the calorimetric cell, in order to determine ΔH_{obs} (Eq. 22). The non-linear least squares fit of the experimental data to the Michaelis-Menten equation for determining the hydrolysis parameters (K_m= 687 μM, k_{cat}= 0.12 s^{-1}) is shown in the right side of thermogram.

4.4.2 Evaluation of kinetic reactions associated to a binding process

Generally, the binding of a ligand to a macromolecule occurs due to different types of non-covalent interactions such as hydrogen bonds, van der Waals, π-stacking, electrostatic …. Thus, the affinity and the energetic for the binding process are intrinsically related with the nature, strength and number of those interactions. The observed heat in a thermogram is a global value of all the contributions taking place simultaneously. It is of outmost importance to determine which processes are contributing to the observed heat and to correct for them, if needed, in order to get the value of the intrinsic binding enthalpy. A particular case occurs when the binding process is followed by a covalent reaction. In those cases, the calorimetric signals will be the result of the two processes: binding and covalent reaction. The analysis of the calorimetric thermograms results in those cases more complicated and for this reason is avoided in the interaction studies. As a result it is difficult to find study cases in the literature. Our description will be based in the study of the interaction of diuretic ethacrynic acid (EA) with the enzyme hGSTP1-1 in phosphate buffer at pH 7 and 25 ºC (Quesada-Soriano et al., 2009). We demonstrated that EA (inhibitor and substrate of hGSTP1-1) binds irreversibly to the α2 loop Cys 47. Fig. 5 shows a representative thermogram.

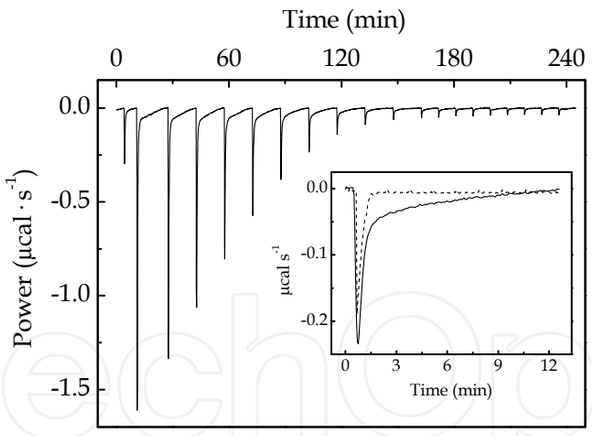

Fig. 5. Calorimetric thermogram for the titration of 23 μM wt GSTP1-1 with 5 μL injections (1 μL first injection) of 2.1 mM EA in 20 mM sodium phosphate, 5 mM NaCl and 0.1 mM EDTA at pH 7.0 and 25ºC. Inset plot: Comparison between a peak from a calorimetric thermogram for the titration of wt enzyme with EA, reflecting the slow kinetic process caused by covalent modification (solid line) and a representative calorimetric trace of a typical binding peak in the absence of a kinetic process (dashed line).

Fig. 5 reveals important differences when comparing the thermogram corresponding to a typical binding titration to one with a concomitant kinetic process. The calorimetric responses after each injection of ligand (peaks in the thermogram) show at least two exothermic phases clearly differentiated by their response times. The response time for the

first phase, ~2 min (comparable to the response time either of a typical binding or a dilution experiment) is smaller than that obtained for the second phase (~12 min). Therefore, the presence of these two phases reveals the occurrence of two sequential and separable steps in the binding reaction. The first process (fast) could be the binding of EA to the protein and the second one could correspond to a chemical reaction (slow) occurring concomitant to the binding process.

The analysis of this thermogram can be done by applying a theoretical model that adequately describes the results from an ITC instrument with feedback system. The capacity to correctly predict the response of the calorimeter to any given thermal effect can allow us to satisfactorily analyze the obtained thermogram. We demonstrated that for an isothermal calorimeter with dynamic power compensation (feedback system) and a similar configuration as used here (VP-ITC from Microcal), the response function to a power pulse (W_0) of finite duration (ξ) can be expressed by the Eq. 24,

$$W(t) = \frac{W_0}{\tau_S - \tau_Q}\left[\tau_S e^{-(t-\xi)/\tau S} - \tau_Q e^{-(t-\xi)/\tau Q} - (\tau_S e^{-t/\tau S} - \tau_Q e^{-t/\tau Q})\right] \quad (24)$$

where, if $t<\Delta t$, then $\xi=t$, and if $t\geq \Delta t$, then ξ becomes constant and equal to Δt (García-Fuentes et al., 1998). τ_S and τ_Q are the response times for the sample cell and the assembly sample cell-feedback system, respectively. It is also worth noting that each injection (peak) displayed in the thermogram in Fig. 5, includes ligand dilution, which always occurs in any binding experiment. Moreover, the possible proton exchange should be also included in each injection. However, since the buffer used is phosphate which has a small ionization enthalpy, the possible protonation/deprotonation effects may be negligible. If the behaviour for each individual process (binding, chemical and dilution) is represented by Eq. 24, the signal generated by each ligand injection will be composed by three contributions:

$$W_g(t) = W_{binding}(t) + W_{chemical}(t) + W_{dilution}(t) \quad (25)$$

By subtracting the dilution trace by a blank experiment, the resultant thermogram will include now only two processes and the generated global power ($W_g(t)$) in each injection will be:

$$W_g(t) = W_{binding}(t) + W_{chemical}(t) \quad (26)$$

where,

$$W_{binding}(t) = \frac{W_{0,b}}{\tau_{S,b} - \tau_Q}\left[\tau_{S,b} e^{-(t-\xi)/\tau S,b} - \tau_Q e^{-(t-\xi)/\tau Q} - (\tau_{S,b} e^{-t/\tau S,b} - \tau_Q e^{-t/\tau Q})\right] \quad (27)$$

$$W_{chemical}(t) = \frac{W_{0,c}}{\tau_{S,c} - \tau_Q}\left[\tau_{S,c} e^{-(t-\xi)/\tau S,c} - \tau_Q e^{-(t-\xi)/\tau Q} - (\tau_{S,c} e^{-t/\tau S,c} - \tau_Q e^{-t/\tau Q})\right] \quad (28)$$

Eq. 26 has six parameters to fit: W_0 and τ_S for the binding process (denoted as $W_{0,b}$ and $\tau_{S,b}$ in Eq. 27);W_0 and τ_S for the chemical process (denoted as $W_{0,c}$ and $\tau_{S,c}$ in Eq. 28); ξ (injection duration) and τ_Q (characteristic time constant for the instrument and therefore, independent of the process occurring in the cell). $\tau_{S,b}$ and τ_Q should be equal to those obtained in the

dilution experiment. This is also true for ξ, because the volume and duration time of the injections are the same in both experiments. On the basis of this empirical procedure, we developed a computational algorithm to fit the individual calorimetric peaks contained in the thermograms obtained from titration at each temperature. Firstly, the peaks from the dilution experiment were used to obtain those three parameters (i.e. $\tau_{S,dilution}=\tau_{S,b}$; $\tau_{Q,\ dilution}=\tau_Q$; ξ), which are then included as fixed values in Eq. 26. This way, each peak in the calorimetric thermogram originated from titrating the protein with the ligand is fitted to Eq. 26 after subtracting the corresponding dilution peak in the reference experiment, obtaining the remaining three parameters: $W_{0,c}$, $W_{0,b}$ and $\tau_{S,c}$.

Fig. 6 shows, as an example, the theoretical deconvolution for a peak from Fig. 5. The two contributions included in Eq. 27, binding and chemical reaction, are visualized as dashed and dotted lines, respectively.

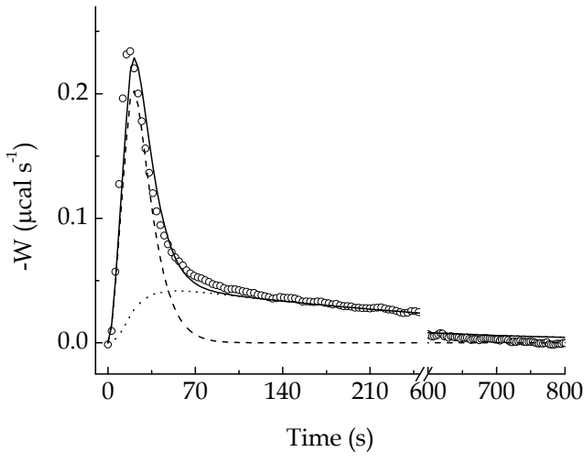

Fig. 6. Schematic example of the theoretical deconvolution procedure for a calorimetric peek of Fig. 5. Solid, dash and dot lines correspond to global signal, binding contribution and kinetic contribution, respectively.

The same deconvolution was applied at all the peaks in the calorimetric trace, and as a result two thermograms are generated. The binding thermogram was used to calculate the binding parameters with the proper model (in this case, two equal and independent sites). Lastly, the kinetic constant for the chemical reaction at this temperature can be calculated from the response time, $\tau_{S,c}$, as $k=1/\tau_{S,c}$.

5. Evaluation of protonation effects in binding processes

The calorimetric enthalpy measured (ΔH_{obs}) is the sum of different heat effects taking place during any reaction. Thus, for instance, if a kinetic reaction involves the release (or uptake) of protons, ΔH_{obs} will be a combination of the reaction intrinsic enthalpy, ΔH_{rxn}, and the protonation (or ionization) enthalpy for each proton absorbed (or released) by the buffer. For instance, the hydrolysis reaction of dUTPase is accompanied by a release of protons, which will be absorbed by the buffer. If the same experiment is done under the same solution conditions but using different buffers with different a protonation enthalpies, the peaks in the traces will have different areas. Fig. 7 shows such a case for the PfdUTPase/dUTP reaction in glycerophosphate, Pipes, Mes, Hepes and TES buffers.

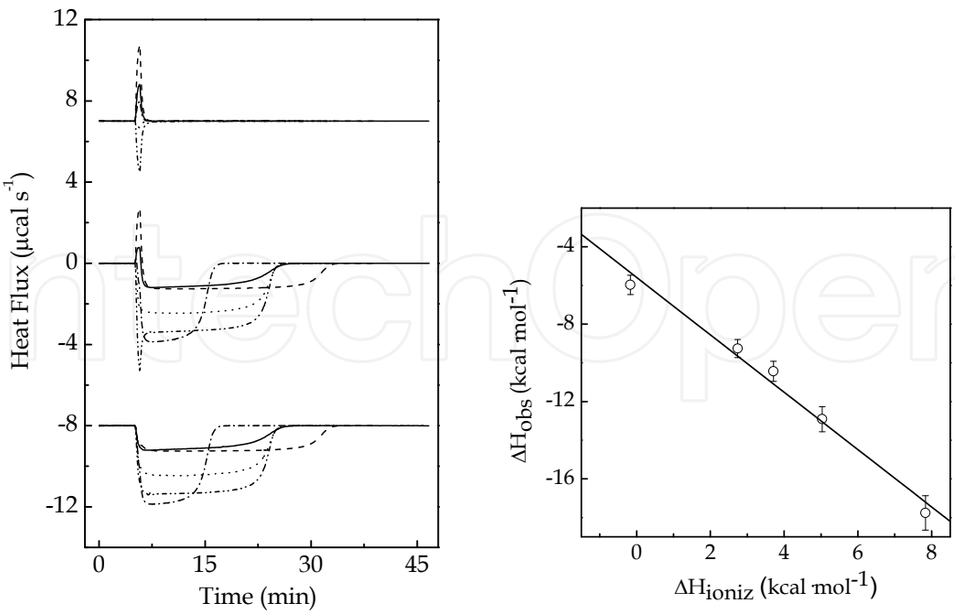

Fig. 7. Protonation effect in the dUTP hydrolysis by PfdUTPase at pH 7 and 25 °C. The calorimetric thermograms correspond to one 20 μL injection of 9.98 mM dUTP to the calorimetric cell containing PfdUTPase (5.5 nM) in (solid line) glycerophosphate, (dash line) Pipes, (dash dot line) Mes, (dot line) Hepes and (dash dot dot line) TES. Upper, medium and bottom panels correspond to the calorimetric traces for dUTP dilution, protein titration and net (protein titration minus dUTP dilution), respectively. Right figure correspond to the fitting to Eq. 29 of the observed reaction enthalpy change, ΔH_{obs}, obtained in each buffer system, *versus* the ionization enthalpy.

$$\Delta H_{obs} = \Delta H_{rxn} + n_H \Delta H_{ioniz} \tag{29}$$

Thus, the enthalpy change of this hydrolysis reaction, ΔH_{rxn} can be calculated from the linear relationship between ΔH_{obs} and the ionization enthalpy, ΔH_{ioniz} (Eq. 29). The intercept gives a ΔH_{rxn} of -5.58 ± 0.52 kcal/mol, and the slope being the number of protons exchanged during the hydrolysis reaction, n_H: -1.48 ± 0.12. In many cases these linked effects are crucial for understanding an enzyme mechanism.

Similarly to a kinetic reaction, whenever binding is coupled to changes in the protonation state of the system, the measured heat signal will contain the heat effect due to ionization of buffer (Baker & Murphy, 1996). Therefore, the observed enthalpy changes (ΔH_{obs}) derived from binding isotherms, are not solely contributed to by the physical forces governing the protein–ligand interactions, but they often contain contributions from the ionization enthalpy of the buffer species and/or changes in the protein conformations. Although the enthalpic contributions from protein conformational changes can be taken as an integral component of the overall binding process, the enthalpic contributions due to protonation changes of the buffer species must be subtracted from the observable. Repeating the calorimetric experiment at the same pH in buffers of different ΔH_{ioniz} allows to determine the number of protons n_H that are released ($n_H>0$) or taken up ($n_H< 0$) by the buffer, and thus to calculate the intrinsic binding enthalpy corrected for protonation heats using a similar relationship to Eq. 29.

6. Case studies

6.1 Thermodynamics of binding to a protein and mutant

A great amount of molecular recognition studies are directed to investigate the binding or affinity of a series of ligands or drugs, with similar structure, to a target protein. The comparative studies with mutants of that protein help to find the role of individual residues both in the catalytic mechanism and in the binding mode. Two examples will illustrate this. Complete thermodynamic profiles consisting of free energy, enthalpy and entropy changes can be obtained for the reactions of interest by calorimetric techniques. The thermodynamic parameters calculated allow to know both the nature of binding site and the functional groups of the ligand that are important for the interaction to occur. This information is very valuable in drug design and cannot be obtained from structural or computational methods alone.

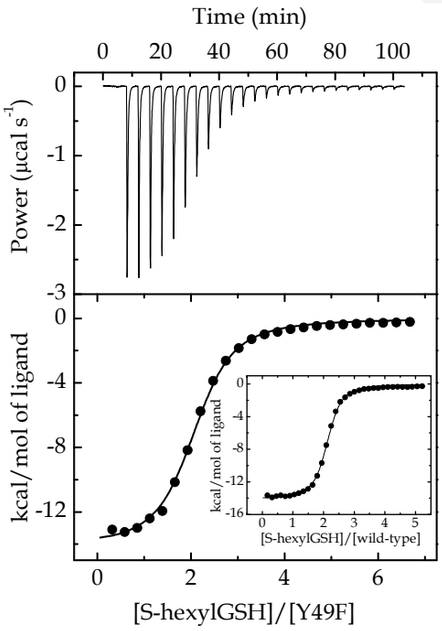

Fig. 8. Representative isothermal titration calorimetry measurements of the binding of S-hexylGSH to the Y49F mutant of hGST P1-1. A 15.32 µM mutant enzyme solution was titrated with 1.12 mM S-hexylGSH. (inset) Integrated heats per mol of S-hexylGSH injected into a solution of wild-type enzyme. 32.66 µM wild type was titrated with 1.31 mM S-hexylGSH.

In the first example we show the thermodynamics of binding of the substrate glutathione (GSH) and the competitive inhibitor S-hexylglutathione to the wt-enzyme and the Y49F mutant of the human glutathione S-transferase (hGST P1-1) (Ortiz-Salmerón et al., 2003). Structural studies revealed that two residues (Cys 47 and Tyr 49) located in a mobile helix, denoted as α2, could participate in intersubunit communication between active sites of the dimer. Fig. 8 shows a representative titration of the Y49F mutant with S-hexylGSH in phosphate buffer at pH 6.5.

6.1.1 Protonation state change

Calorimetric titration experiments were repeated in various buffers of different ΔH_{ioniz} (phosphate, MOPS, MES and ACES) at pH 6.5 and 25 °C. The binding enthalpy, ΔH and the number of exchanged protons were obtained from the intercept and slope of a linear plot

according to Eq. 29 (Table 1). A negative slope was obtained ($n_H < 0$), with n_H ~-0.44 and n_H~-0.11 for the binding of GSH to the wild type enzyme and its Y49F mutant, respectively (Table 1).

		Y49F mutant		Wild-type	
		GSH	S-hexylGSH	GSH	S-hexylGSH
Buffer	ΔH_{ioniz} (kcal mol^{-1})	$-\Delta H_{obs}$ (kcal mol^{-1})		$-\Delta H_{obs}$ (kcal mol^{-1})	
Phosphate	1.22	13.04 ± 0.31	17.14 ± 0.33	9.91 ± 0.19	16.13 ± 0.26
Mes	3.72	-	-	11.27 ± 0.31	15.58 ± 0.42
Mops	5.27	13.48 ± 0.33	16.55 ± 0.41	11.67 ± 0.23	-
Aces	7.53	13.74 ± 0.40	15.41 ± 0.25	12.71 ± 0.32	16.20 ± 0.45
n_H		-0.11 ± 0.01	0.24 ± 0.09	-0.44 ± 0.08	-0.02 ± 0.01

Table 1. Protonation effect.

Hence, upon enzyme-GSH complex formation, the number of protons released for the wild-type enzyme binding was higher than that for the Y49F mutant. This means that one or more pK_a values, corresponding to some donor proton groups in the ligand and/or enzyme, decrease (i.e. become more acidic). Although n_H indicates the global number of protons uptaken or released upon ligand binding, it is usually the result of only one or two residues changing their protonation state. Since ~-0.45 H^+/monomer are released in the wild-type/GSH binding, but the number is practically zero for the binding of the S-hexylGSH inhibitor to the wild-type hGSTP1-1, the protons released during the binding of substrate (GSH) to the wild-type enzyme might come from the thiol group of the sulfhydryl in GSH. However, there exists a net concomitant uptake of protons for the formation of the S-hexylGSH-Y49F complex (n_H~0.25) (Table 1). The results for the Y49F mutant were explained by assuming that the mutation induces slight changes in the environment of the binding site, producing a pK_a shift in one or more groups of the ligand and/or enzyme upon complex formation. In this case, it cannot be assumed that only the sulfhydryl group in GSH is responsible for the proton exchange at this pH, since the binding of S-hexylGSH to Y49F should therefore take place without a proton exchange, which was contrary to our results. Overall the following could be deduced: 1) the proton of the thiol group of GSH is released upon binding to both the Y49F mutant and wild-type anzymes; and 2) upon binding of GSH to the mutant, at least two groups participate in the proton exchange: the sulfhydryl group in GSH and a second group with a low pK_a capable of increasing its pK_a as a consequence of binding. This second group takes up ~0.25 protons from the buffer media. Whereas an unambiguous assignment of the specific residue(s) responsible for the binding-induced uptake of protons is not possible, the side chains of Asp and Glu are likely candidates as ionizing groups at pH 6.5. Crystallographic studies showed that the Asp 98 of the adjacent subunit is located at the active site. This residue (pK_a=4.8), involved in a hydrogen-bonding network around the γ-glutamate of GSH or S-hexylGSH, could increase its pK as a consequence of a small local conformational change arising from the mutation, thus explaining the number of protons taken up in the association with these ligands.

6.1.2 Temperature dependence

When an ITC experiment is carried out at several temperatures the heat capacity change of the reaction can be obtained from the enthalpy dependence on temperature. Fig. 9 shows the

dependency of the thermodynamic parameters on temperature for the wild-type enzyme and its Y49F mutant. The binding of these ligands to both enzymes is noncooperative within the temperature range analyzed, which suggests that the interaction does not induce a conformational change affecting the binding of the second ligand molecule to the other site of the dimer.

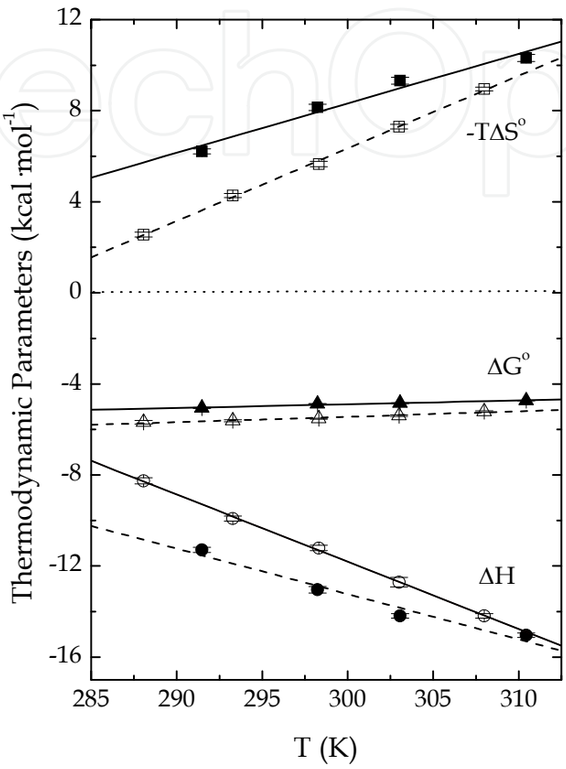

Fig. 9. Temperature dependence of the thermodynamic parameters for the binding of GSH to both the Y49F mutant (filled symbols) and the wild-type (open symbols) enzyme.

ΔG^0 is almost insensitive to the temperature change, in both cases, but increases as a consequence of the mutation, so the ligand affinity (GSH and S-hexylGSH) for Y49F is lower than for the wild-type enzyme. This behavior was observed at all the temperatures studied (Fig. 9). This result alone could also be obtained from other techniques, such as fluorescence. However, ITC is able to split the affinity values into the enthalpic and entropic contributions, allowing for a deeper understanding of the binding process.

Protein	Ligand	K	ΔH	$T\Delta S^o$	ΔC_p^o
		M^{-1}	kcal mol^{-1}		cal K^{-1} mol^{-1}
WT	GSH	11630±302	-11.21±0.12	-5.65±0.12	-294.2±2.7
Y49F	GSH	3883±83	-13.04±0.14	-9.17±0.14	-199.5±26.9
WT	S-hexylGSH	(8.1±0.3) ·10^5	-16.13±0.07	-8.04±0.07	-441.6±48.7
Y49F	S-hexylGSH	(4.3±0.1) ·10^5	-17.14±0.08	-9.45±0.08	-333.6±28.8

Table 2. Thermodynamic parameters for the interaction of GSH and S-hexylGSH to the Y49F mutant and wild-type enzymes of hGST P1-1, at 25.2ºC and pH 6.5.

As shown in Fig. 9, although ΔG^0 is almost insensitive to the change in temperature, ΔH and $T\Delta S^0$ strongly depend on it, for both enzymes. This feature is known as enthalpy-entropy compensation, and it is very common in most of the thermodynamic binding studies of biological systems.

The enthalpy-entropy compensation is related to the properties of the solvent as a result of perturbing weak intermolecular interactions. In Fig. 9 a linear dependence of ΔH with the temperature was observed, from the slope of which the heat capacity change (ΔC_p^o) upon ligand binding was obtained. The absolute values of ΔC_p^o calculated for the binding of either substrate or S-hexylGSH to the mutant Y49F decreased ~100 cal K^{-1} mol^{-1} when compared to those for the wild-type enzyme. This is most probably due to a different release of water molecules from both complexes, being the number of water molecules released by the wt-ligand complex higher than in the mutant-ligand case. The release of water molecules is accompanied by an increased entropy change. This suggestion for the ΔC_p^o difference is supported by a comparison between the entropy change values for both enzymes (Table 2), since it is slightly higher for the wild-type at all temperatures (Fig. 9). The data reported here indicate that, thermodynamically, the mutation leads to increased changes in negative enthalpy and negative entropy (Table 2 and Fig. 9). Although the interaction between the Y49F mutant and GSH is enthalpically more favorable than that for wild-type enzyme, the entropic loss due to binding is also increased, indicating that the mutation is both enthalpically favorable and entropically unfavorable (Table 2). The same tendency was obtained for the binding of S-hexylGSH. This means that the thermodynamic effect of this mutation is to decrease the entropic loss due to binding. The unfavorable entropy change outweighs the enthalpic advantage, resulting in a 3-fold lower binding constant for the binding of GSH to the wild-type enzyme. Also, compared to GSH, S-hexylGSH shows more negative values for the two contributions (enthalpic and entropic), maybe as a consequence of the higher apolarity in the inside of the active site provided by the hexyl chain of this inhibitor. This also could explain its higher affinity.

6.1.3 Correlation between ΔC_p and the buried surface area

Works carried out during the last decade supports the view that the changes in the thermodynamic quantities associated with the folding and ligand-binding processes can be parametrized in terms of the corresponding changes in nonpolar (ASA_{ap}) and polar (ASA_p) areas exposed to the solvent (in $Å^2$ units). Thus, Freire and co-workers (Murphy & Freire, 1992) have suggested the following equations for the ΔC_p and the enthalpy change (at the reference temperature of 60 ^oC (this temperature is taken as a reference because it is the mean value of the denaturation temperatures of the model proteins used in the analysis).

$$\Delta C_p = 0.45\Delta ASA_{ap} - 0.26\Delta ASA_{pol} \tag{30}$$

$$\Delta H_{60} = -8.44\Delta ASA_{ap} + 31.4\Delta ASA_{pol} \tag{31}$$

Therefore, from an experimentally determined ΔC_p and a measured enthalpy change at 25 ^oC, the corresponding enthalpy change at 60^oC is calculated by $\Delta H_{60}=\Delta H_{25}+\Delta C_p$ (60-25). If we admitted Eqs. 30 and 31 to be valid for binding processes, we would have a two equation system with two unknowns from which we could calculate changes in accessible surface

areas. Changes in apolar (ΔASA_{ap}) and polar (ΔASA_p) solvent-accessible surface areas upon complexation have been estimated by those relationships mentioned above. On the basis of the X-ray crystallographic data of several proteins, the changes in the water-accessible surface areas of both nonpolar (ΔASA_{ap}) and polar (ΔASA_p) residues on protein folding have been calculated. Such calculations reveal that the ratio $\Delta ASA_{ap}/\Delta ASA_p$ varies between 1.2 and 1.7. This range is comparable with the medium value for the ratio of $\Delta ASA_{ap}/\Delta ASA_p$ of ~1.2, calculated for the interactions described in this study. The application of Murphy's approach (Murphy & Freire, 1992) to the experimentally determined values indicates that the surface areas buried on complex formation comprise ~54% of the nonpolar surface. Therefore, as Spolar and Record (1992) indicate, these values can be taken as the "rigid body" interactions, and therefore, no large conformational changes occur as a consequence of the association with these ligands. On the other hand, Eq. 30 can also be used to obtain an estimation of the ΔC_p value for a generic macromolecule-ligand interaction, under the assumption that this parameterization is valid for binding processes. In those cases, structural information should be available for the complex as well as for the interacting species. In general, changes in solvent-accessible surface area (ΔASA) are determined as the difference in ASA between the final and initial states. For a molecular interaction process, this is the difference between the ASA for the complex and the sum of the ASA for the macromolecule and the ligand, resulting in negative values of ΔASA. ΔASA is further subdivided into nonpolar and polar contributions by simply defining which atoms take part in the surface. The original description is based on the Lee and Richards (1971) algorithm implemented in software NACCESS (Hubbard & Thornton, 1996), using a sphere (of solvent) of a particular radius to 'probe' the surface of the molecule. There is a high number of other parameterizations used also to determine ASA. However, since each implementation yields slightly different results, it is very important to assure the implemented parameters when performing calculations.

6.2 Application of calorimetry to predict the binding mode of a ligand

Frequently, as it has been described before, negative ΔC_p values are usually attributed to the burial of apolar groups from water. However, in many systems it is also thought to be associated with hydrophobic stacking interactions, presumably resulting from the dehydration of highly ordered water molecules surrounding hydrophobic surfaces. In order to describe in more detail this observation we will show two examples.

6.2.1 Binding of EASG to wt and Y108V mutant of hGSTP1-1

The EASG is a conjugate of ethacrynic acid (with aromatic groups) and reduced glutathione (tripeptide). The thermodynamic parameter values obtained are shown in Table 3. As it can be observed, the thermodynamic parameter values are very similar, the main difference being the absolute ΔC_p values, which were considerably larger (approximately twice as large) for the binding to the Y108V mutant when compared to the wt enzyme.

These results might be used to make an assessment on the predilection of the Y108V mutant to adopt a particular 3D structure, when it is complexed with EASG, where there is a high drop in the centroid distance between the ligand EA moiety and Phe 8. This analysis is based on the assumption that the overall conformation of the Y108V mutant complexed with

EASG is relatively unchanged from that of the wt protein and that the main effect is the π-stacking between the EA and flanking aromatic amino acids such as Phe 8 located in the active site. Thus, the more negative value of ΔC_p was interpreted as coming from a strengthening of the π-stacking between the EA moiety and Phe 8 in the absence of Tyr 108. This increase in the strength of a particular π-π interaction in the Y108V mutant explained the larger negative ΔC_p value for the interaction with it compared to the wt enzyme. These results were corroborated by the X-ray crystallography of this free mutant and its complex with EASG.

Protein	K_d (μM)	ΔH (kcal mol^{-1})	TΔS^0 (kcal mol^{-1})	ΔC^0_p (cal mol^{-1}K^{-1})
WT	0.5 ± 0.1	-14.17 ± 0.37	-5.59 ± 0.37	-264 ± 24
Y108V	0.3 ± 0.1	-13.34 ± 0.46	-4.55 ± 0.31	-415 ± 17

Table 3. Thermodynamic parameters of the interaction of EASG with wt GST P1-1 and theY108V mutant at 25 ^{o}C and pH 7.0

Therefore, these results demonstrate that ITC measurements can provide a thermodynamic fingerprint of drug–protein interactions, which can be related to the molecular mode of binding in multimeric enzymes. Calorimetric data can therefore be a useful method to complement X-ray crystallographic studies. However, even in the absence of structural information, thermodynamics can give a guideline to improve drug potency. Reports of comparisons of drug binding energies with relevant structural studies are still rather scarce in the literature. Thus, studies such as ours are of great general interest.

6.2.2 Binding of S-benzylglutathione to GST from *Schistosoma japonicum*

When X-Ray data are not available for a particular macromolecule-ligand complex, but there is enough structural knowledge about the ligand binding modes of similar ligands to the same or similar proteins, the combination of ITC thermodynamic data with docking studies may predict the preferred binding mode or pose of the ligand under study in the complex.

As an example, we have carried out the thermodynamic studies of the binding of S-benzylglutathione to the GST from *Schistosoma japonicum* (wt-SjGST) and three important Tyr 111 mutants (Y111L, Y111T and Y111F), because this residue has an active role in the enzyme activity (to be published).

The ΔC_p values for the interaction of this ligand with wt-SjGST and the Y111F, Y111L and Y111T mutants were -733, -745, -576 and -499 cal mol^{-1}K^{-1}, respectively, within a 20-40 ^{o}C range.

From these ΔC_p values it is clear the interaction of the ligand with the wt and the Y111F mutant must proceed in a similar fashion, whereas the thermodynamic data show the interaction with the Y111L and Y111T mutants has been altered compared to the wt.

Following the previous reasoning relating ΔC_p values to a change in π-stacking interactions, and taking into account the structural knowledge and ligand binding modes of this protein (Cardoso et al., 2003), it is not illogical to think the difference in the ΔC_p values might come from a lacking π-stacking interaction between the benzyl moiety of the ligand and the aromatic ring of the 111 residue in the active site in the case of the Y111L and Y111T mutants. To address this question we carried out a series of docking studies with AutoDock

Vina (Trott & Olson, 2010), where the ligand was docked to the wt and its three mutants, which were built with the "Mutagenesis Wizard" in PyMOL from the wt structure (The PyMOL Molecular Graphics System, Version 1.3.1_pre3925, Shrödinger, LLC). Fig. 10 (PyMOL) superimposes the two best docked poses for S-benzylglutathione in the active site for the four enzymes, as well as the binding mode of the very similar S-2-iodobenzylglutathione as a reference (pdb structure 1M9B, Cardoso et al., 2003).

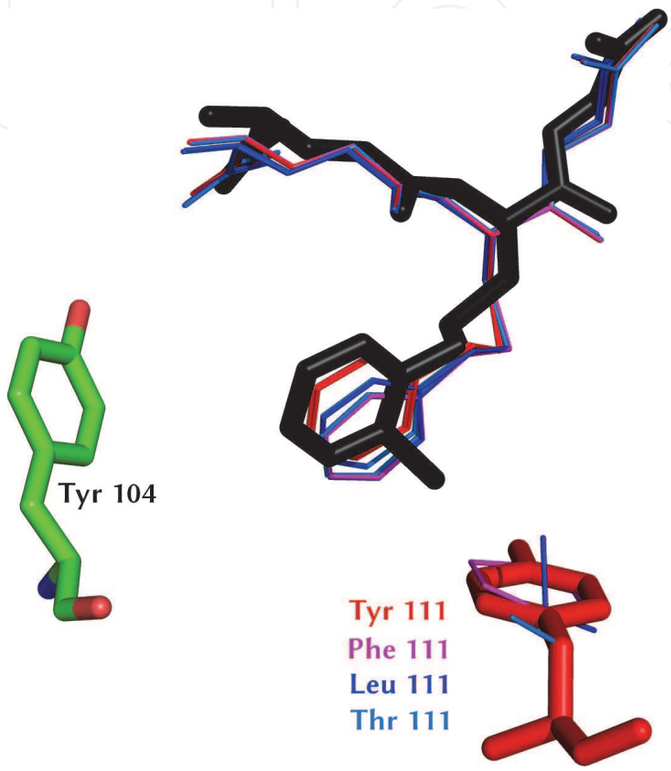

Fig. 10. Two best docked poses of S-benzylglutathione in the active site of wt SjGST (red) and its three mutants: Y111F (magenta), Y111L (blue) and Y111T (light blue). Only the relevant 104 and 111 residues are displayed. S-2-iodobenzylglutathione (black) from the PDB structure 1M9B is shown as a reference.

	Angle (Tyr 104)	Centroid distance (Tyr 104)	Angle (res. 111)	Centroid distance (res. 111)
Reference [a]	50.0º	6.6 Å	80.8º [b]	6.6 Å
wt	58.2º	6.9 Å	73.9º [b]	6.5 Å
Y111F	59.2º	7.4 Å	73.5º [c]	6.3 Å
Y111L	60.0º	7.3 Å	-	-
Y111T	59.3º	7.2 Å	-	-

Table 4. Mean geometric data for the interaction between the S-benzylglutathione ring plane and the Tyr 104 and residue 111 ring planes. [a]S-2-iodobenzylglutathione from the PDB structure 1M9B. [b] wt Tyr 111. [c]Phe 111

The predicted S-benzylglutathione binding modes agree with the crystallographic structure for this reference ligand (Table 4), where the aromatic ring of the benzyl moiety stacks between the side-chains of Tyr 104 and Tyr 111 in the case of the wt and the Y111F mutant, but stacks only against Tyr 104 in the case of the Y111L and Y111T mutants. We propose the lacking π-stacking interaction against the side-chain of residue 111 in these two mutants is responsible for the difference in the ΔC_p measured.

7. Conclusions

In the beginning of this chapter we stated thermodynamics can help us understand how life works. We hope the reader has now a better understanding why we did so. Among the available thermodynamic techniques to address the question, Isothermal Titration Calorimetry is perhaps the most powerful tool at our disposal. Apart from being a universal technique, not only does it provide us with the crucial affinity between two interacting species, but it also allows us to know the reason for it. By splitting the affinity into enthalpic and entropic contributions, and after combining the thermodynamic parameters with the structural knowledge available or molecular modeling predictions, the individual interactions responsible for the recognition between a ligand and a macromolecule emerge. This information is of the utmost importance for a rational drug design against a desired target. Last but not least, ITC can even be used for kinetic studies. It is able to detect weak enzyme activity under situations where the traditional spectrophotometric method fails, as we demonstrated. In fact, it is even possible to detect a covalent bonding in the cases where the binding process under study is followed by an unexpected chemical reaction, a situation impossible to properly address with other titration techniques. We have shown how to find out the thermodynamic and kinetic parameters from a single ITC trace in this case.

8. Acknowledgments

Research in the authors' laboratory is supported by grants CTQ2010-17848 from Spanish Plan Nacional , Ministerio de Ciencia e Innovación (co-financied by FEDER) and FQM-3141 and CVI-6028 from the Andalusian Region, Junta de Andalucía (Spain).

9. References

Baker, B.M. & Murphy, K.P. (1996) Evaluation of linked protonation effects in protein binding reactions using isothermal titration calorimetry. *Biophys. J.* 71, 2049 – 2055.

Cardoso, R.M.F.; Daniels, D.S.; Bruns, C.M. & Tainer, J.A. (2003) Characterization of the electrophile binding site and substrate binding mode of the 26-kDa glutathione S-transferase from *Schistosoma japonicum*. *Proteins*, 51, 137-146.

Freire, E. ; Schön, A. & Velazquez-Campoy, A. (2009) Isothermal titration calorimetry: general formalism using binding polynomials. *Methods Enzymol.* 455, 127-55.

García-Fuentes, L. ; Barón, C. & Mayorga. O.L. (2008) Influence of dynamic power compensation in an isothermal titration microcalorimeter. *Anal. Chem*. 70, 4615-23.

Hilser, V.J. ; Gómez, J. & Freire, E. (1996) The enthalpy change in protein folding and binding: Refinement of parameters for structure-based calculations. *Proteins* 26, 123–133.

Horn, J. R. ; Russell, D.M. ; Lewis, E.A. & Murphy, K.P. (2001) Van' t hoff and calorimetric enthalpies from isothermal titration calorimetry: Are there significant discrepancies?. *Biochemistry* 40, 1774 – 1778.

Hubbard, S.J. & Thornton, J.M. (1996) NACCESS Computer Program. 2.1.1 ed. London: Department of Biochemisry & Molecular Biology, University College.

Lee, B. & Richards, F.M. (1971) The interpretation of protein structures: estimation of static accessibility. *J. Mol. Biol.*; 55, 379–400.

Murphy, K. P. & Freire, E. (1992) Thermodynamics of Structural Stability and Cooperative Folding Behavior in Proteins. *Adv. Protein Chem.* 3, 313–361.

Ortiz-Salmerón, E. ; Nuccetelli, M. ; Oakley, A.J. ; Parker, M.W. ; Lo Bello, M. & García-Fuentes, L. (2003) Thermodynamic description of the effect of the mutation Y49F on human glutathione transferase P1-1 in binding with glutathione and the inhibitor S-hexylglutathione. *J. Biol. Chem*. 278, 46938-48.

Quesada-Soriano, I. ; Casas-Solvas, J.M. ; Recio, E. ; Ruiz-Pérez, L.M. ; Vargas-Berenguel, A. ; González-Pacanowska, D. & García-Fuentes, L. (2010) Kinetic properties and specificity of trimeric *Plasmodium falciparum* and human dUTPases. *Biochimie* 92,178-86.

Quesada-Soriano, I. ; Leal, I. ; Casas-Solvas, J.M. ; Vargas-Berenguel, A. ; Barón, C. ; Ruíz-Pérez, L.M. ; González-Pacanowska, D. & García-Fuentes, L. (2008) Kinetic and thermodynamic characterization of dUTP hydrolysis by *Plasmodium falciparum* dUTPase. *Biochim. Biophys. Acta.* 1784, 1347-55.

Quesada-Soriano, I. ; Musso-Buendia, J.A. ; Tellez-Sanz, R. ; Ruíz-Pérez, L.M. ; Barón, C., González-Pacanowska, D. & García-Fuentes, L. (2007) *Plasmodium falciparum* dUTPase: studies on protein stability and binding of deoxyuridine derivatives. *Biochim. Biophys. Acta* 1774, 936-45.

Quesada-Soriano, I. ; Parker, L.J. ; Primavera, A. ; Casas-Solvas, J.M. ; Vargas-Berenguel, A. ; Barón, C. ; Morton, C.J. ; Mazzetti, A.P. ; Lo Bello, M. ; Parker, M.W. & García-Fuentes, L. (2009) Influence of the H-site residue 108 on human glutathione transferase P1-1 ligand binding: structure-thermodynamic relationships and thermal stability. *Protein Sci.* 18, 2454-70.

Spolar, R.S. ; Livingstone, J.R. & Record, M.T. (1992) Coupling of local folding to site-specific binding of proteins to DNA. *Biochemistry* 31, 3947–3955.

Téllez-Sanz, R. ; Cesareo, E. ; Nuccetelli, M. ; Aguilera, A.M. ; Barón, C. ; Parker, L.J. ; Adams, J.J. ; Morton, C.J. ; Lo Bello, M. ; Parker, M.W. & García-Fuentes, L. (2006) Calorimetric and structural studies of the nitric oxide carrier S-nitrosoglutathione bound to human glutathione transferase P1-1. *Protein Sci.* 15, 1093-105.

Todd, M.J. & Gomez, J. (2001) Enzyme kinetics determined using calorimetry: a general assay for enzyme activity?. *Anal. Biochem.* 296, 179–187.

Trott, O. & Olson, A.J. (2010) AutoDock Vina: Improving the speed and accuracy of docking with a new scoring function, efficient optimization, and multithreading. *J. Comput. Chem.* 31, 455-461.

Velazquez-Campoy, A. & Freire, E. (2006) Isothermal titration calorimetry to determine association constants for high-affinity ligands. *Nature Protocols*, 1, 186-191.

Wiseman, T. ; Williston, S. ; Brandts, J. F. &Lin, L.-N. (1989) Rapid measurement of binding constants and heats of binding using a new titration calorimeter. *Anal. Biochem.* 179, 131 – 137.

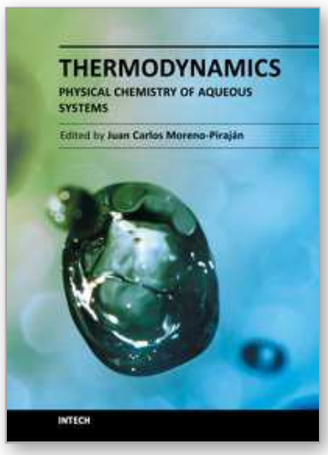

Thermodynamics - Physical Chemistry of Aqueous Systems

Edited by Dr. Juan Carlos Moreno PirajÃ¡n

ISBN 978-953-307-979-0
Hard cover, 434 pages
Publisher InTech
Published online 15, September, 2011
Published in print edition September, 2011

Thermodynamics is one of the most exciting branches of physical chemistry which has greatly contributed to the modern science. Being concentrated on a wide range of applications of thermodynamics, this book gathers a series of contributions by the finest scientists in the world, gathered in an orderly manner. It can be used in post-graduate courses for students and as a reference book, as it is written in a language pleasing to the reader. It can also serve as a reference material for researchers to whom the thermodynamics is one of the area of interest.

How to reference

In order to correctly reference this scholarly work, feel free to copy and paste the following:

Luis Garcîa-Fuentes, Ramiro, Téllez-Sanz, Indalecio Quesada-Soriano and Carmen Barón (2011). Thermodynamics of Molecular Recognition by Calorimetry, Thermodynamics - Physical Chemistry of Aqueous Systems, Dr. Juan Carlos Moreno PirajÃ¡n (Ed.), ISBN: 978-953-307-979-0, InTech, Available from: http://www.intechopen.com/books/thermodynamics-physical-chemistry-of-aqueous-systems/thermodynamics-of-molecular-recognition-by-calorimetry

INTECH
open science | open minds

InTech Europe
University Campus STeP Ri
Slavka Krautzeka 83/A
51000 Rijeka, Croatia
Phone: +385 (51) 770 447
Fax: +385 (51) 686 166
www.intechopen.com

InTech China
Unit 405, Office Block, Hotel Equatorial Shanghai
No.65, Yan An Road (West), Shanghai, 200040, China
中国上海市延安西路65号上海国际贵都大饭店办公楼405单元
Phone: +86-21-62489820
Fax: +86-21-62489821

IntechOpen